

Clusters AgeS Experiment. Hot subdwarfs and luminous white dwarf candidates in the field of the globular cluster M4¹

B. J. Mochejska, J. Kaluzny

Copernicus Astronomical Center, Bartycka 18, 00-716 Warszawa

mochejsk@camk.edu.pl, jka@camk.edu.pl

I. Thompson

Carnegie Observatories, 813 Santa Barbara Street, Pasadena, CA 91101, USA

ian@ociw.edu

W. Pych

Copernicus Astronomical Center, Bartycka 18, 00-716 Warszawa

pych@camk.edu.pl

ABSTRACT

We present *UBV* color magnitude diagrams (CMDs) for the globular cluster M4. The CMDs show a sequence of four luminous blue stars ($V < 20$, $U - V < -0.6$) which appear to be cluster hot subdwarfs. We present spectra for the three brightest ones. We also note the presence of a population of faint blue objects, likely to be hot, young white dwarfs (WDs) belonging to the cluster. We have selected five objects above $V = 22$ mag, bright enough for follow-up ground-based spectroscopy and present their coordinates and finding charts. We show a spectrum for variable V46 (Kaluzny et al. 1997) which suggests that it is a hot subdwarf, along with a new light curve obtained with the ISIS image subtraction package (Alard 2000). The light curve is unstable, but only one period of variability is apparent. Two new variables have been discovered, both located on the cluster red giant branch (RGB). We also present a differential $E(B - V)$ reddening map and a fiducial sequence for the main sequence, subgiant branch and red giant branch on the $V/B - V$ CMD for a selected region with uniform reddening. Based on a comparison with the M5 fiducial sequence we obtain a reddening estimate of $E(B - V) = 0.41$ mag towards M4, consistent with previous determinations.

Subject headings: globular clusters: individual (M4) – Hertzsprung-Russell diagram – stars: subdwarfs – stars: white dwarfs

1. Introduction

The Clusters AgeS Experiment (CASE) is a long term project with the main goal of determining accurate ages and distances to globular clusters using detached eclipsing binaries (Paczynski 1997). The photometry of new eclipsing binaries

in M4 has already been presented by Kaluzny et al. (1997). In this paper we investigate the presence of blue stars in the field of the M4 globular cluster: hot blue subdwarfs and young bright white dwarfs (WD).

Recently several metal-rich globular clusters have been found to possess a handful of blue subdwarfs (Rich et al. 1997). Several scenarios have been proposed to explain the formation of such

¹Based on observations collected at the Las Campanas Observatory 2.5m du Pont telescope.

objects (Moehler 2001). The study of the properties of these stars could shed some light on the mechanisms of their creation. Only one such star, Y453 (Cudworth & Rees 1990), has been reported to date in M4.

The globular cluster M4 = NGC 6121 ($\alpha_{2000} = 16^h 23^m 36^s$, $\delta_{2000} = -26^\circ 31' 32''$) is the nearest globular cluster. Due to its proximity M4 has been the subject of searches for WDs in the past. Several WD candidates were found by Chan and Richer (1986) in a blink survey designed to select ultraviolet-excess objects. Drukier, Fahlman & Richer (1989) presented the spectra of two of those objects. One was found to be a very hot subdwarf (sdO) and the other a field DA with weak hydrogen lines. Recently a large sample of WDs has been identified with the HST (Richer et al. 1995; 1997).

Our *UBV* photometry, although inferior in depth to that obtained with the HST, covers a much larger area of M4 and thus offers a possibility to uncover new young bright WD candidates at the top of the cooling sequence, located in less crowded regions. Such objects would be within the reach of ground-based spectroscopy. The study of these objects could provide further constraints on stellar evolution models of WD progenitors. Our photometry also covers the entire central part of the cluster, not investigated in the Chan & Richer blink survey.

This paper is organized as follows: in Section 2 we describe the observations. Section 3 outlines the data reduction procedure. In Section 4 we provide details of the calibration of our instrumental magnitudes to the standard system. In Section 5 we present and examine the color-magnitude diagrams (CMDs) constructed from our *UBV* photometry. In Subsections 5.1 and 5.2 we describe the luminous hot subdwarfs and the WD candidates, respectively. A differential reddening map and a fiducial sequence for the $V/B - V$ CMD are presented in Subsections 5.3 and 5.4. In Subsection 5.5 we determine the value of the reddening $E(B - V)$ towards M4. We discuss the variable V46 in Section 6 and present two new variables in Section 7. Section 8 contains the concluding remarks.

2. Observations

The photometric data were obtained with the 2.5 m du Pont telescope at Las Campanas Observatory, equipped with a thinned 2048×2048 Tektronix CCD with a scale of $0''.26 \text{ pixel}^{-1}$. An $8'.8 \times 8'.8$ field centered on the cluster was monitored during five consecutive nights, from June 1st to 5th, 1995. Observations were made through Johnson *UBV* filters. Most of the frames were collected in the *B* band, with exposure times varying slightly with the observing conditions, typically 120s in *B* and 60s in *V*. The average seeing was $1''.1$. Newly discovered variables were presented in Kaluzny et al. (1997). A more detailed description of the collected data is presented therein.

Spectra of the blue subdwarfs B1, B2 and B3 were obtained at the Baade 6.5 m telescope with the Boller & Chivens spectrograph equipped with Tek#1 CCD. The wavelength coverage extends from 3774 to 4492 Å at a resolution of 0.7 Å. Two spectra were taken for each of the stars, on May 8th, 2001 for B1 (500 s) and B2 (600 s) and on June 16th and 19th, 2001 for B3 (1200 s). The spectra were combined to increase the signal to noise ratio (S/N) which ranged from ~ 16 to ~ 23 for single exposures.

A 30-minute 6.3 Å resolution spectrum of V46, extending from 3753 to 6961 Å was obtained on the night of April 25th, 1996 with the 3.6m ESO telescope using the EFOSC1 spectrograph.

3. Data reduction

The photometry was carried out using Daophot/Allstar (Stetson 1994). The positional variability of the point-spread function was modeled with a second order approximation. The extraction of profile photometry closely followed the procedure described in Mochejska & Kaluzny (1999).

The *V* band photometry was obtained from an image combined from three 300 s exposures with subarcsecond seeing. The images were transformed to a common coordinate system using the ISIS image subtraction package (Alard 2000) and median combined with IRAF² using an averaged

²IRAF is distributed by the National Optical Astronomy Observatories, which are operated by the Association of Universities for Research in Astronomy, Inc., under cooperative agreement with the NSF.

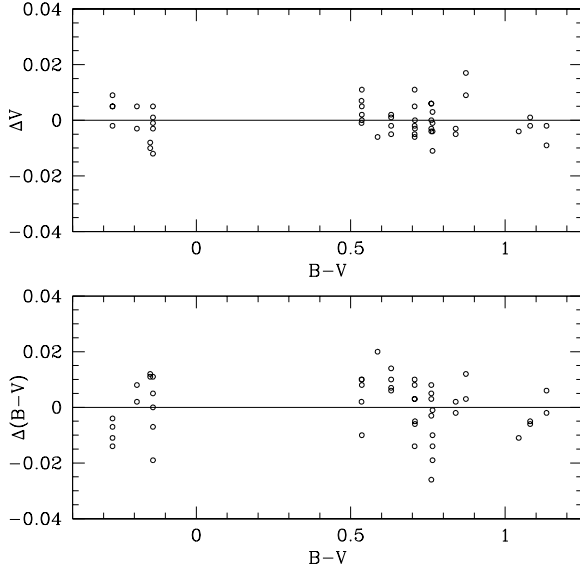


Fig. 1.— V and $B - V$ residuals of Landolt standard stars as a function of $B - V$ resulting from transformations defined by Eqs. (5)-(6).

sigma clipping algorithm to reject cosmic rays. To recover some of the saturated stars, the photometry from an averaged 3×60 s image, a 20 s and a 6 s exposure was included. A similar approach was followed for the U and B band data. The final U band photometry was derived from a median combined 4×900 s image and a 480 s exposure. For the B band we used an averaged 2×800 s image, a median combined 3×120 s image and a 30 s exposure. The full list of exposures used in the construction of the CMD is provided in Tab. 1.

The photometry lists derived from the images for each filter were transformed to a common instrumental system defined by the longest exposure in each filter. Saturated stars were removed from the long exposures. From the shorter exposure lists we removed stars fainter than the magnitude at which the average formal error on the short exposure was twice the error on the longest exposure. In the final step the lists were added, with the best of the available measurements (i.e., having the smallest formal error) retained for stars present on more than one list. In addition we removed 24 RR Lyrae variables from the photometry lists.

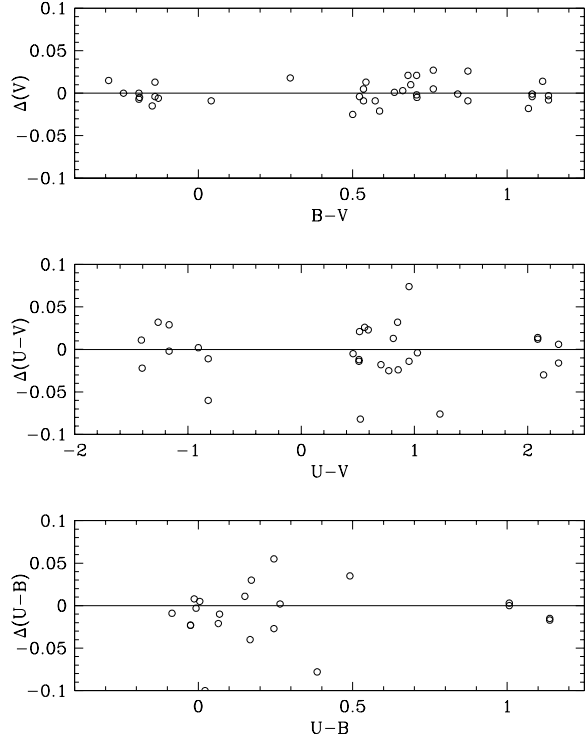


Fig. 2.— V , $U - B$ and $U - V$ residuals of Landolt standard stars as a function of color resulting from transformations defined by Eqs. (7)-(10).

4. Calibration

The color terms of the transformations of instrumental magnitudes to the standard system were derived from 19 observations of Landolt (1992) fields collected on 5 nights spread between April 22/23 and June 3/4, 1995. The same instrumental setup (CCD+filters) was used on all nights. The following values were obtained by averaging color terms derived for separate nights:

$$v = V - 0.0160(B - V) + c_1 \quad (1)$$

$$b - v = 0.9440(B - V) + c_2 \quad (2)$$

$$u - b = 0.9480(U - B) + c_3 \quad (3)$$

$$u - v = 0.9450(U - V) + c_4 \quad (4)$$

The constant offsets for V and $B - V$ were determined relative to M4 data collected with the same telescope on the night of May 31/June 1 1998 at airmasses of 1.07-1.11. The transformation coefficients were derived from 56 stars in 6 Landolt fields observed that night at airmasses

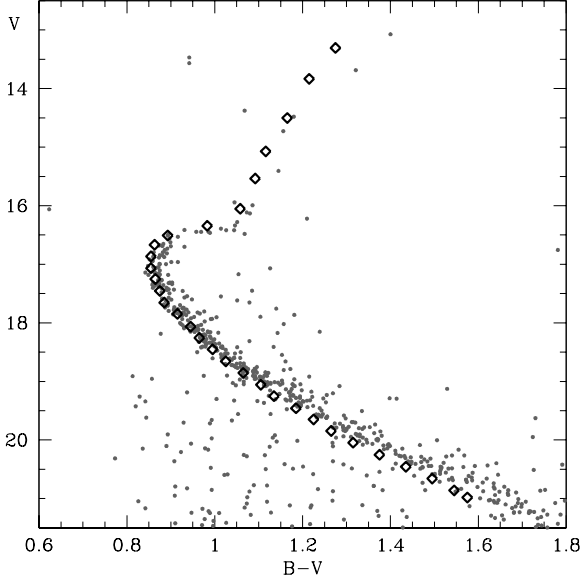


Fig. 3.— A comparison of our BV photometry with the photometry of Alcaïno et al. (1997). Fiducial points determined from our data (diamonds) are overlaid on the Alcaïno et al. CMD (points).

ranging from 1.07 to 1.75. Figure 1 shows the residuals of the standard stars resulting from the following transformations:

$$v = V + 0.6903 - 0.0176 \cdot (B - V) \quad (5)$$

$$b - v = 0.3057 + 0.9507 \cdot (B - V) \quad (6)$$

The offsets for $U - B$ and $U - V$ were determined from a comparison with M4 data collected with the 1m Swope telescope at LCO at airmasses less than 1.06. We observed 39 stars in 9 Landolt fields at airmasses ranging from 1.07 to 1.36. The extinction coefficients were assumed as the average values for the winter season at LCO. The following transformations were adopted:

$$v = V + 2.7837 - 0.0189(B - V) + 0.15(X - 1.25) \quad (7)$$

$$b - v = 0.3058 + 0.9359(B - V) + 0.12(X - 1.25) \quad (8)$$

$$u - b = 2.0252 + 0.9377(U - B) + 0.31(X - 1.25) \quad (9)$$

$$u - v = 2.3269 + 0.9313(U - V) + 0.44(X - 1.25) \quad (10)$$

Figure 2 shows the V , $U - B$ and $U - V$ transformation residuals of the standard stars.

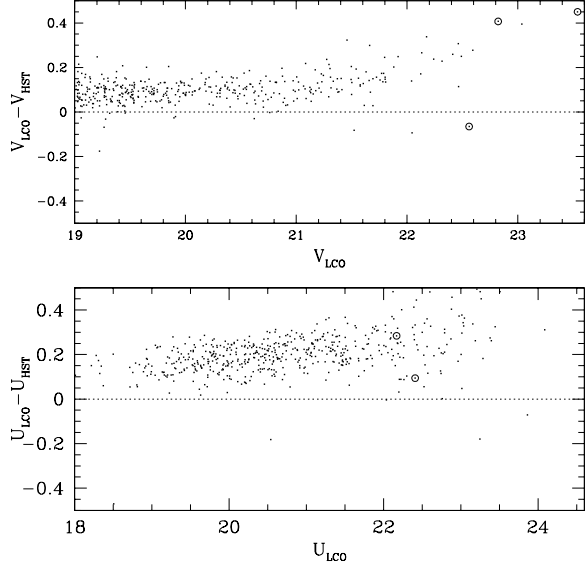


Fig. 4.— A comparison of our UV photometry with the HST photometry of Ibata et al. (1999). WDs are marked with open circles.

As a check of consistency of the V and $B - V$ transformations we have compared the May 31/June 1 1998 calibrated M4 data (Eqs. (5) and (6)) with the June 1995 data transformed to the standard system using the color terms in Eqs. (1) and (2) and offsets relative to the transformations given by Eqs. (7) and (8). For stars with $V < 16$ mag the offsets in V and $B - V$ are -0.026 and -0.020 mag, respectively. There is no correlation between the residuals and color.

We have compared our $V/B - V$ diagram with a CMD constructed from the photometry obtained by Alcaïno et al. (1997) in a $6' \times 6'$ field bordering our field on the west (data courtesy of Dr N. Samus). As Alcaïno et al. report the existence of a reddening gradient across the face of the cluster, with the reddening increasing to the west, we selected for the comparison the westernmost $2'2 \times 8'8$ and easternmost $2' \times 6'$ sections of our and Alcaïno et al. fields, respectively. We fitted fiducial points to the two datasets in the magnitude range $16.8 < V < 20$. The mean offset between the two sequences is -0.007 mag. In Figure 3 we overplot the Alcaïno et al. $V/B - V$ CMD with fiducial points fitted to our data.

In Figure 4 we compare our UV photometry with that obtained with the HST (Ibata et al.

1999; Richer et al. 1997). The offsets in the photometry are 0.095 mag in V and 0.129 in U for stars with $19 < V < 21$ mag and $18 < U < 22$ mag, respectively. A similar systematic offset between ground-based and HST V magnitudes has been noted by Richer et al. (1997; Figure 2 therein). For stars above $V = 20$ mag the difference in photometry dramatically increases with magnitude.

5. Color-magnitude diagrams

The $V/B - V$, $V/U - B$ and $V/U - V$ color-magnitude diagrams (CMD) constructed from our data are presented in Figure 5. The CMDs exhibit a well defined main sequence that can be traced down to $V \simeq 22$ mag on the $V/B - V$ CMD and $V \simeq 21$ mag on the remaining two diagrams. The subgiant, red giant and horizontal branches are well populated, but there are few stars on the asymptotic giant branch. The horizontal branch exhibits a clear RR Lyrae gap. A sequence of four luminous blue stars is present on the CMDs (plotted as open triangles). These objects are discussed in more detail in Subsection 5.1. There is also a population of faint blue stars with magnitudes and colors ($V < 21$ mag, $U - V < 0.4$ mag) consistent with the values expected for the upper part of the white dwarf cooling sequence. A brief discussion of these objects is presented in Subsection 5.2. In Subsections 5.3 and 5.4 we present a differential reddening map and a sequence of fiducial points determined for the $V/B - V$ CMD. In Subsection 5.5 we estimate the reddening $E(B - V)$ towards M4.

5.1. Hot subdwarfs

We note a sequence of four luminous blue stars on the CMDs ($V < 20$, $U - V < -0.6$), most probably hot subdwarfs belonging to the cluster (marked with triangles on the CMDs in Figure 5). The brightest of these, B1, was initially discovered by Cudworth & Rees (1990; Y453 in their catalog). No other stars as blue as these were found in a blink survey aimed at the detection of UV excess objects in an area between $3^{\circ}9'$ and $23^{\circ}7'$ from the cluster center (Chan & Richer 1986). Four bright blue objects with $V < 20$ and $U - V < -0.1$ were found in that study: 1710 (reported as non-stellar), 774, 1285 and 710 (see Table 2 therein).

The star 774 was investigated spectroscopically by Drukier et al. (1989) and found to be most likely a field WD. One fainter object, 831 with $V = 20.33$ and $U - V = -0.97$ was found to be a very hot subdwarf by Drukier et al. (1989).

In Figure 6 we present the spectra of B1, B2 and B3, smoothed with a boxcar filter 5 units in length. Helium lines are indicated with continuous lines and hydrogen lines with dotted ones. B1 (Y453) has been previously studied spectroscopically by Moehler, Landsman & Napiwotzki (1998). Their analysis indicates that it could be a post-early asymptotic giant branch (PEAGB) star with $T_{eff} = 58800$ K. Our spectrum shows broad Balmer lines, but the He I and He II lines reported in the Moehler et al. (1998) data are barely discernible, most likely due to our higher resolution and moderate S/N. B2 shows singly and doubly ionized helium lines. The lines at wavelengths corresponding to the hydrogen Balmer series are most likely due to doubly ionized helium, judging by the presence of the He II line at 4200 \AA . It appears to be a very hot helium rich subdwarf, approximately sdO5:He4 in the Jeffery et al. (1997) classification scheme. The precise classification is somewhat uncertain, as it is based on only three lines in the 300 \AA overlap between our and their spectra: the He II line at 4339 \AA and He I lines at 4388 \AA and 4471 \AA . The spectrum of B3 exhibits broad Balmer lines and two lines from singly ionized helium (4026 \AA and 4471 \AA) and none from He II. It appears to be an sdB:He1 subdwarf.

The spectrum of B2, which appears to be helium-rich, is quite unusual. Hot subdwarfs in globular clusters are almost always found to be helium-poor (e.g. Moehler et al. 1997a). Only one hot helium-rich subdwarf in a globular cluster has been reported to date (Moehler et al. 1997b). B2 seems to be only the second such star known. Brown et al. (2001) suggest that such stars might have undergone late helium-core flash while descending the WD cooling sequence. A convection zone produced during the helium flash would mix hydrogen into the hot interior, where it would be consumed, thus greatly enhancing the envelope helium abundance. However, B2 seems to be too luminous for their scenario.

The hot subdwarf B3 and possibly B2 could belong to a vertical extended horizontal branch (EHB), not reported in previous studies of this

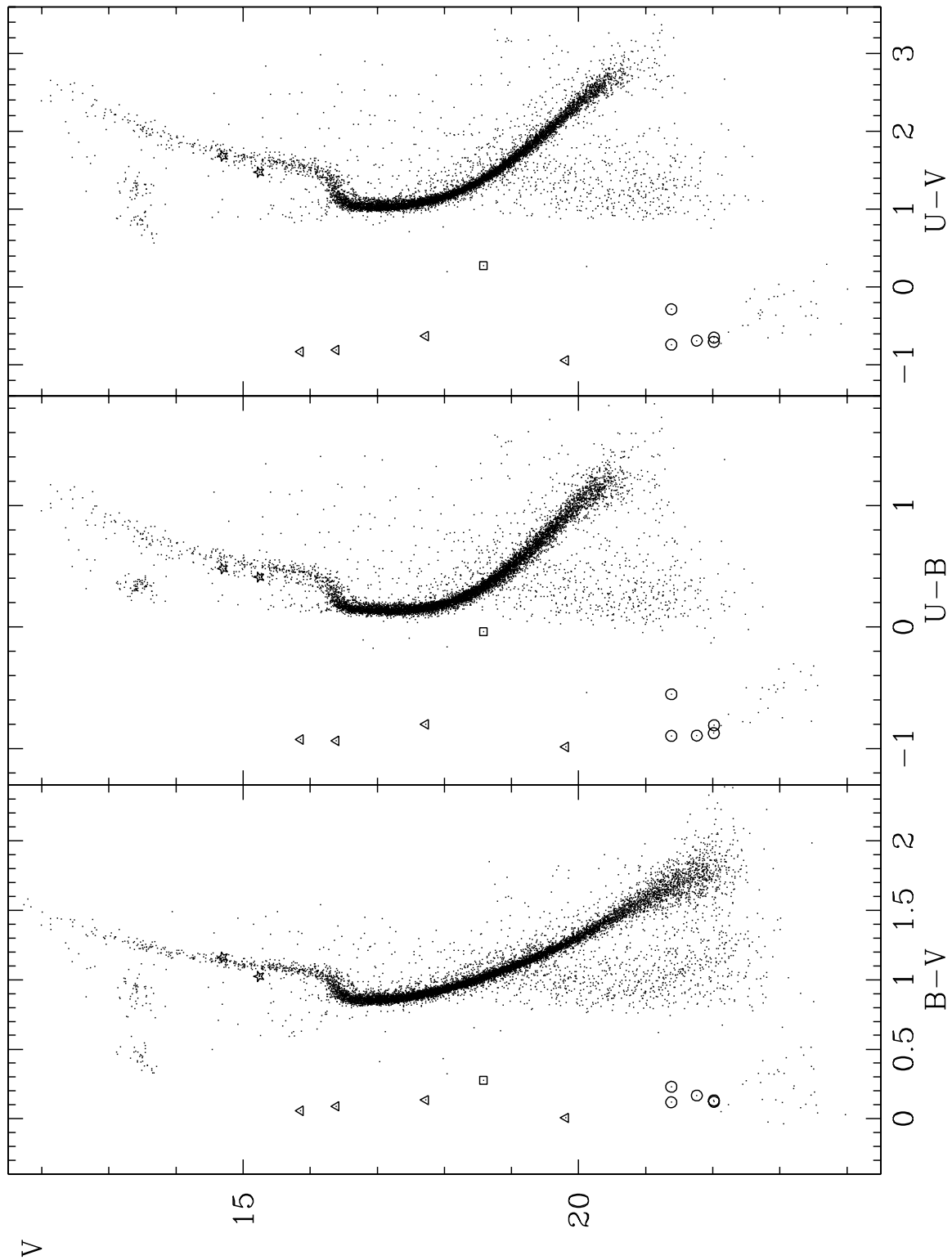


Fig. 5.— The $V/B - V$, $V/U - B$ and $V/U - V$ color-magnitude diagrams of the M4 globular cluster.

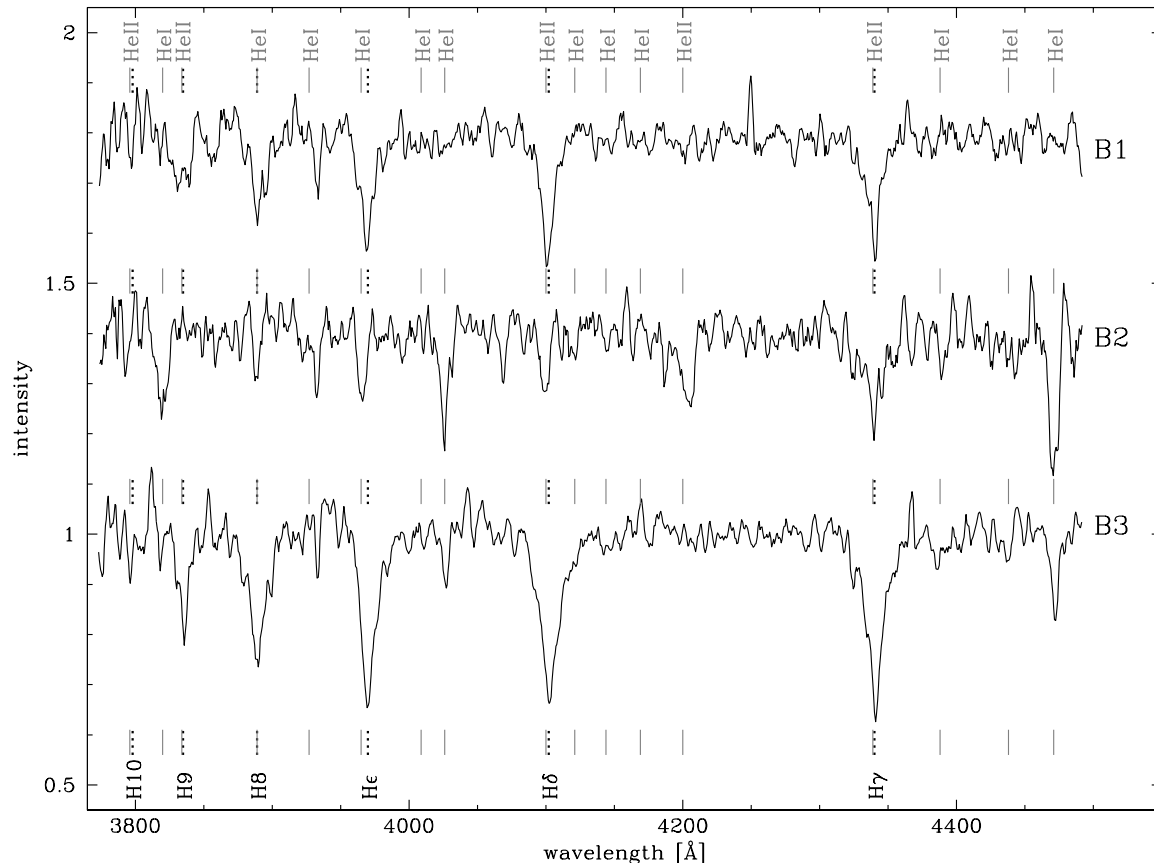


Fig. 6.— The spectra of blue stars B1, B2 and B3, smoothed with a boxcar filter 5 units in length. He I and He II lines are indicated with continuous lines, H I with dotted ones.

cluster. Generally the globular cluster horizontal branch (HB) morphology correlates with metallicity - the HB becomes redder as the mean metal abundance increases. However, variations in HB morphology at a given metallicity are observed and a second, still unknown parameter has to be introduced. It has been suggested that mass loss on the red giant branch may be the second parameter (Catelan 2000). The stars which suffered strong mass loss would become EHB stars (D’Cruz et al. 1996, D’Cruz 1998). Recently the existence of high-metallicity hot blue horizontal branch stars has been reported in the relatively metal-rich globular clusters NGC 1851 (Bellazzini et al. 2001) and 47 Tuc (Ferraro et al. 2001), the very old metal-rich open cluster NGC 6791 (Kaluzny & Udalski 1992) and the Milky Way bulge (Peterson et al. 2000). Detailed study of the nature of such extreme horizontal branch stars could provide valu-

able clues regarding the unknown second parameter.

An alternative explanation for B4 is that it is a low-mass helium WD. Similar stars have been identified in the globular cluster NGC 6397 (Cool et al. 1998) and the spectrum of one of them was found to be consistent with a He WD (Edmonds et al. 1999). Using differential surface density data from HEQS (Köhler et al. 1997), LBQS (Hewett et al. 1995) and the 2dF QSO survey (Boyle et al. 2000) we estimate the probability of B4 being a quasar to be between 2% and 48%.

We have checked the subdwarf candidates for variability in our observations spanning 5 days and found them to be constant within the errors of the photometry.

In Table 2 we list the photometry and equatorial coordinates for the hot subdwarfs. Finding

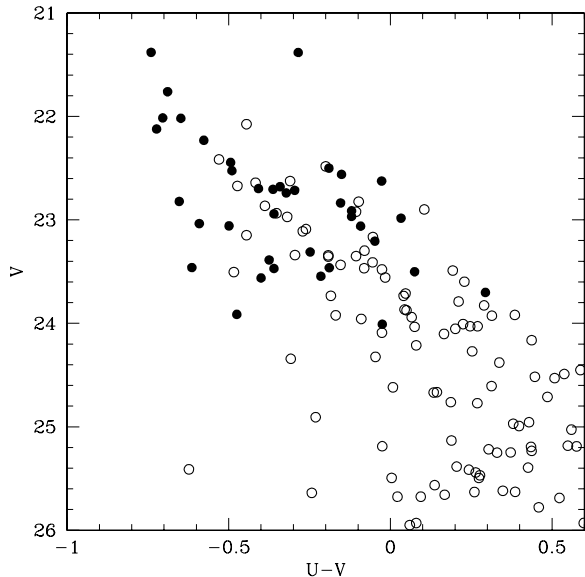


Fig. 7.— A $V/U - V$ CMD showing our white dwarfs (filled circles) and those discovered with the HST by Richer et al. (1997, open circles).

charts for these stars are presented in Figure 14. Each chart covers $33'' \times 33''$ on the sky.

5.2. White dwarf candidates

A population of faint blue stars is present on our CMDs. In Figure 7 we overplot these stars (filled circles) with the WDs observed with the HST (open circles, Richer et al. 1997). Their location is consistent with the upper part of the HST white dwarf cooling sequence. Figure 4 is a comparison of our UV photometry and that of the HST, open circles indicate WDs that are common to the two studies.

The photometry and equatorial coordinates for the five brightest objects with $V \lesssim 22$ (marked with open circles in Figure 5) are presented in Table 3³ and $33'' \times 33''$ V and U band finding charts are presented in Figure 13. These objects are located in the outer, less crowded regions of the cluster (compared to the HST WD sample) and are bright enough for ground-based spectroscopy.

³The full table is available from the authors via anonymous ftp from [cfa-ftp.harvard.edu](ftp://cfa-ftp.harvard.edu/pub/bmochejs/M4/) in the directory /pub/bmochejs/M4/

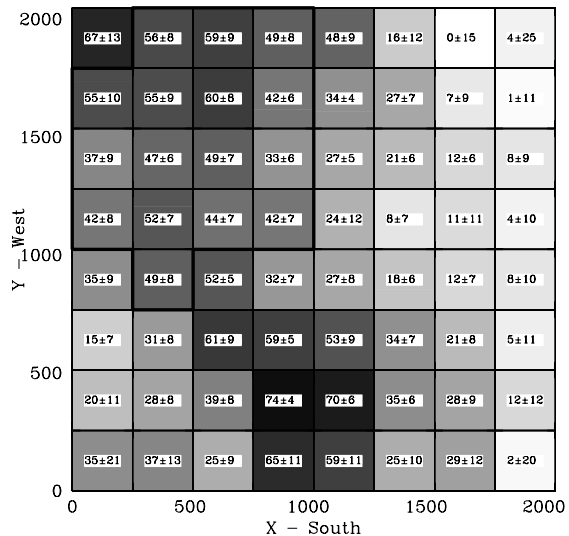


Fig. 8.— The differential reddening map for 64×64 subfields covering the field of M4. The differential reddening is given in millimagnitudes measured relative to the section with the lowest reddening. Higher values of $\delta E(B - V)$ correspond to higher reddening. The region used in the determination of the fiducial sequence is shown surrounded with a thick line. The cluster center is located approximately at $(X_C, Y_C) = (1100, 1000)$.

5.3. Differential Extinction Map

All of the principal sequences on the CMDs display a broadening due to the differential reddening across the face of the cluster, as discussed by Cudworth & Rees (1990), Fahlman et al. (1996), and Alcaïno et al. (1997). The differential reddening has been investigated by Lyons et al. (1995) using K1 column density measurements towards 16 stars and by Ivans et al. (1999; 2000) on the basis of spectroscopic analysis of 22 red giant branch stars. These studies revealed the existence of a patchy reddening variation across the cluster face. In addition, Peterson, Rees & Cudworth (1995) found evidence for an unusually high value of $R_V = A_V/E(B - V) \approx 4$.

We have constructed an 8×8 element differential reddening map following closely the procedure presented by von Braun & Mateo (2000), based on the approach of Kaluzny & Krzemiński (1993). The errors were also derived as described therein,

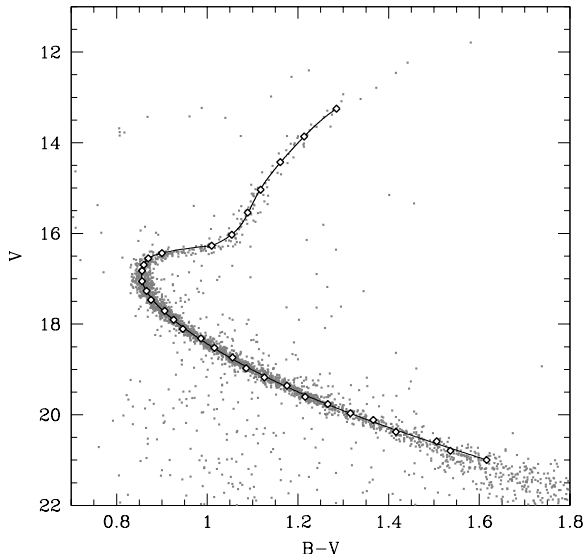


Fig. 9.— The fiducial sequence for the $V/B - V$ CMD in the selected region of M4 with uniform absorption.

taking into account the correlation between the errors in color and magnitude. We adopted $R_V = 4$ in our analysis. Figure 8 presents the derived map of differential reddening, measured relative to the section with the lowest reddening. The extinction appears to be weakest in the east and increases to the west, in accordance with results obtained in previous studies (eg. Alcaïno et al. 1997). The patchy nature of the reddening is also confirmed.

We have compared our differential extinction map with the Schlegel, Finkbeiner & Davis (1998; hereafter SFD) dust map. There is some qualitative similarity between the two maps: both show lowest reddening in the northeastern corner, intermediate in the southwestern and higher in the northwestern corners. The maps disagree as to the reddening in the southeastern section: the SFD map shows the strongest reddening there, while it is rather small on our map. Another difference is that the differential reddening is larger on our map (up to 0.074) than on the SFD map (up to 0.039). We have checked a larger area around M4 on the SFD map and noted that it is located in a region of highly variable extinction. The cluster coincides with the center of a void with patchy lower extinction ($E(B - V) \sim 0.5$) some $1^\circ \times 1^\circ$ surrounded by thick filaments of higher extinction

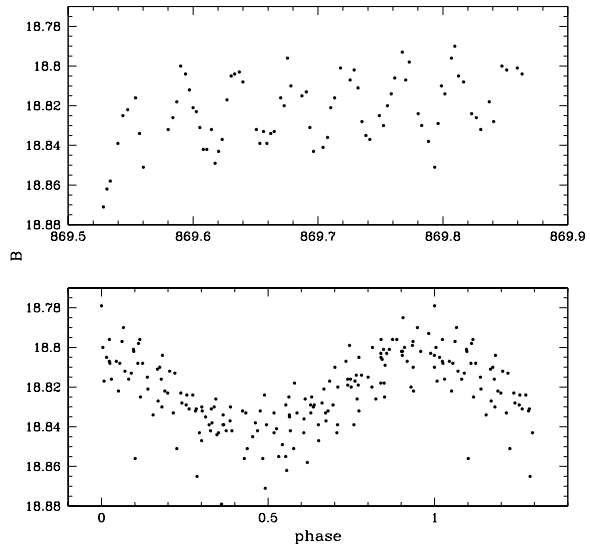


Fig. 10.— The light curve of the hot subdwarf V46. Upper panel: the raw light curve for the first night of observations. Lower panel: light curve from all five nights phased with a period of 0.04358 d

($E(B - V) > 1$ mag). Moreover, we notice that the $E(B - V)$ values from the SFD map range from 0.472 to 0.511 mag for the cluster area, which is substantially higher than the reddening value of $E(B - V) = 0.36$ mag reported for M4 by Harris (1996). This discrepancy might be due to the fact that the SFD map also takes into account the extinction caused by dust located behind the cluster. This interpretation would invalidate to large extent any comparison between the two reddening maps.

5.4. $V/B - V$ CMD Fiducial Sequence

To derive the $V/B - V$ fiducial sequence we have selected a region of uniform reddening using the differential reddening map constructed in Subsection 5.3. This region is shown in Figure 8 surrounded with a thick line. The fiducial points were determined separately for the main sequence (MS; $16.75 < V < 21.0$), the subgiant branch (SGB; $16.2 < V < 16.75$) and the red giant branch (RGB; $13.0 < V < 16.2$). For the MS and SGB, the fiducial points were determined by finding the mode of the color distribution, smoothed with a boxcar filter 0.03 mag in length, in magnitude bins 0.21 and 0.135 mag wide, respectively. The magnitude

for each bin was computed as the mean. In case of the RGB we adopted a different procedure, as this branch is more sparsely populated than the previous two. To avoid contamination of the RGB sample, especially with the AGB and HB stars, the following magnitude-dependent color cuts were applied: $(29.7 - V)/14.5 < B - V < (32.6 - V)/14.5$. For the RGB, the fiducial points were computed as the mean color in magnitude bins 0.55 mag wide. The magnitudes within each bin were determined as the mean, just as for the MS and SGB. The resultant fiducial sequence is presented in Figure 9, superimposed on the CMD which was used in their derivation. The fiducial sequence is listed in Table 4.

5.5. Foreground Extinction $E(B-V)$

We have obtained an independent estimate of foreground extinction in B-V towards M4 from comparison of the fiducial sequence constructed in the previous Subsection with the one given by Sandquist et al. (1996) for the M5 globular cluster. We have chosen M5 for this purpose due to its low reddening ($E(B-V) = 0.03$; Harris 1996), similar metallicity ($[Fe/H] = -1.11$ dex as compared with -1.19 dex for M4; Carretta & Gratton 1997) and similar age ($\tau_{M4} - \tau_{M5} = 0.6$ Gyr; Rosenberg et al. 1999).

To determine the $B - V$ colors of the cluster turnoffs (TO) we fitted the fiducial points in the turnoff regions with a fifth order Chebyshev polynomial. The color of the turnoff was taken as the color of the bluest point on the fitted curve. We obtained the values of 0.854 and 0.470 for M4 and M5, respectively. From the isochrones of Girardi et al. (2000) we estimated the corrections in $(B - V)_{TO}$ for the difference in metallicity (-0.08 dex) and age (0.6 Gyr) between M4 and M5 to be -0.014 and $+0.006$ mag, respectively. Assuming an extinction of 0.03 mag towards M5, we obtain a reddening value of $E(B - V) = 0.41$ for M4. This is consistent with the value of 0.36 listed by Harris (1996), taking into account the variability of the extinction across the face of the cluster. It is in disagreement with the total extinction estimate of 0.5 mag based on the SFD dust maps.

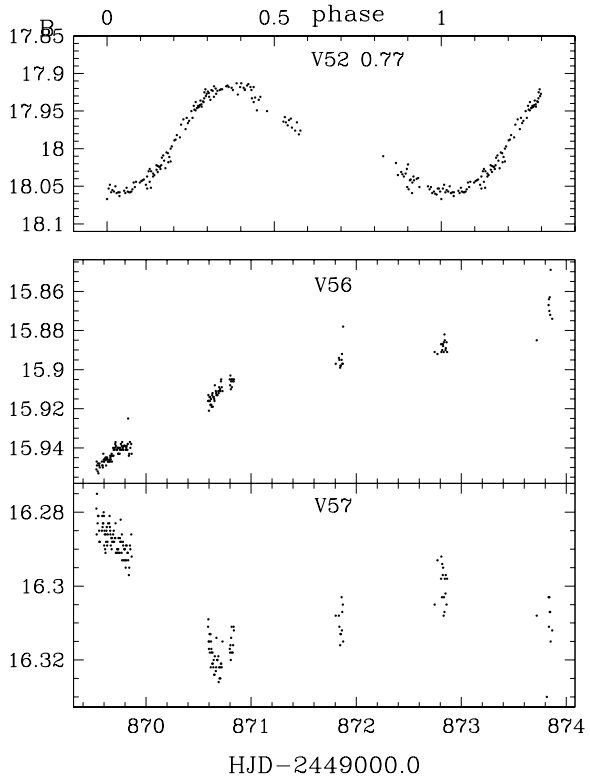


Fig. 12.— The light curves of the variables V52, V56 and V57. The last two variables are newly discovered. V52 is phased with the newly derived period of 0.77d.

6. The variable hot subdwarf V46

V46 was detected to be variable by Kaluzny et al. (1997). The star exhibits coherent modulations with a period of 0.04358 d. It is indicated on the CMDs in Figure 5 with an open square and mean photometry is listed in Table 5. We have measured the light curve of V46 using the ISIS image subtraction package (Alard & Lupton 1998; Alard 2000). The upper panel of Figure 10 shows the raw light curve for the first night of observations. The phased light curve from all five nights is shown in the lower panel. The shape of the light curve appears to be unstable. We have searched for other coherent periodicities and have found none. Nevertheless, we cannot rule out multiple periodicity, due to the short timespan of our observations.

The spectrum of V46, shown in Figure 11, exhibits strong and broad Balmer lines, while the

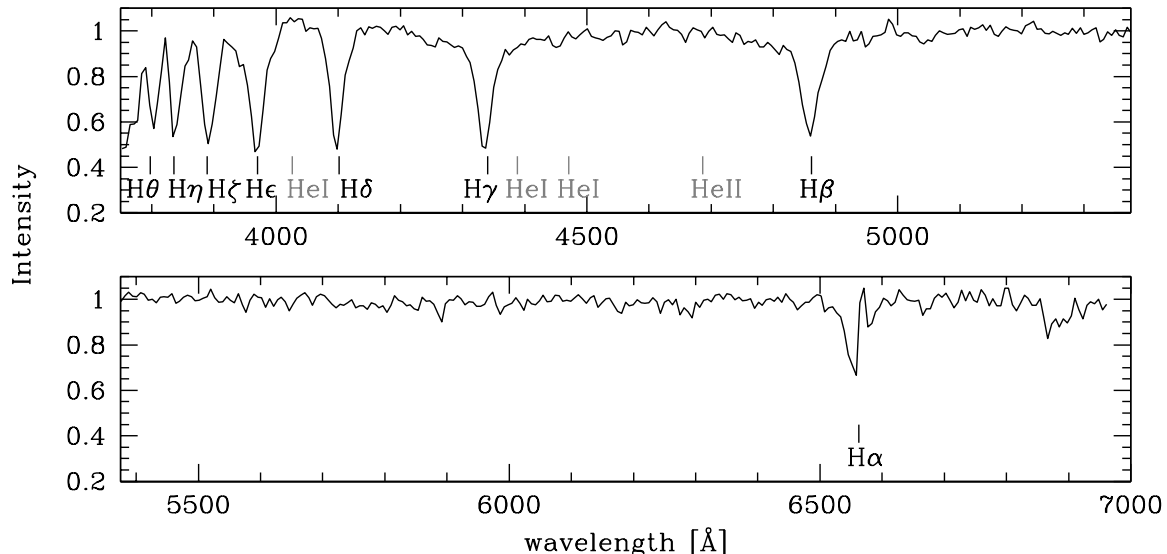


Fig. 11.— The spectrum of the hot subdwarf V46. The hydrogen Balmer series and helium lines are marked and labeled. The wavelengths of the helium lines are as follows: He I(4026Å) He I(4388Å), He I(4471Å), He II(4686Å).

He I and He II lines are absent. We have compared it with spectra for stars of types B through F, taken from the spectral atlas of Pickles (1998). Our spectrum is consistent with types from late B through late A. The dereddened colors $(B - V)_0 = -0.13$ and $(U - B)_0 = -0.32$ suggest V46 is a late B type star. In order to be a main sequence late B star ($M_V \simeq -1.5$), at $V_0 \sim 17.1$ it would have to be located at a distance modulus of ~ 18.6 mag or 52 kpc (assuming the larger $E(B - V) = 0.5$ from Schlegel et al. (1998)). At $b = 15.97$ this corresponds to $Z = 14$ kpc. This suggests that V46 is rather a hot subdwarf, type sdB1 in the Jeffery et al. (1997) classification scheme.

Although the spectrum of V46 indicates that it is an sdB, its period of brightness modulations ($0.04358\text{d}=3765\text{s}$) is much longer than the typical periods of 100-200s (500s in extreme cases) for pulsating subdwarfs (Koen et al. 1998).

Another possibility to consider are AM CVn type interacting binary WD systems. AM CVn itself exhibits a low amplitude flickering light curve with a period of $0.01216\text{d}=1051\text{s}$ (Krzeminski 1972; Provencal et al. 1995). GP Com (G61-29) is the longest period variable of this class, with $P=0.03231\text{d}=2791\text{s}$ (Marsh 1999). However, AM CVn type variables show He I features in their

spectra, accompanied by a lack of hydrogen lines. This is in disagreement with the V46 spectrum and thus renders this interpretation very unlikely.

A different interpretation, also suggested more by the light curve than by the spectrum, is that V46 is a field SX Phe star. Its period is typical for these variables. The light variations appear remarkably similar to those of SX Phe stars (i.e. Breger et al. 1995, Handler et al. 1996, Pych et al. 2001, Kaluzny & Thompson 2001). The location of V46 on the CMD (Fig. 5) would suggest that it should be located behind the cluster.

An alternative interpretation could be that V46 is a binary star with the brightness modulations due to the reflection effect or to ellipsoidal variations ($P=0.08716\text{d}=2.09\text{h}$). A study of the radial velocities of a sample of 70 sdBs indicates that 45% of them are post-common envelope binaries with periods of the order of a few hours to a few days (Saffer, Green & Bowers 2000). The period for V46 is consistent with this period range. Spectra with better time resolution are needed to verify this interpretation.

7. Other variables

The data set was reanalyzed using the ISIS image subtraction package (Alard & Lupton 1998, Alard 2000) mainly with the aim of obtaining a better light curve for V46. The light curves of all previously found variables were also extracted and two new variables were found. There is notable improvement in the quality of the photometry extracted with ISIS, as compared to traditional profile photometry. In Figure 12 we show the new ISIS light curve for the previously discovered variable V52, phased with its newly derived period of 0.7765 days (Tab. 5). The light curves of the two new variables V56 and V57 are also presented in Figure 12, their photometry is listed in Tab. 5 and finding charts are presented in Figure 13. On the CMDs (Figure 5) these variables are located on the RGB (star symbols).

8. Conclusions

Our investigation of the M4 *UBV* color magnitude diagrams has resulted in the identification of four luminous hot subdwarfs (one previously known) and the tip of the white dwarf cooling sequence. The hot blue stars could possibly form a vertical extended horizontal branch of the cluster. The spectra for the three brightest blue stars confirm that they are hot subdwarfs. Further study would be required to elucidate the nature of the fourth object. We have selected five luminous WD candidates above $V \simeq 22$ mag, located in the outer, less crowded regions of M4. These objects would make good targets for follow-up ground-based spectroscopy. In addition we present a fiducial sequence for the $V/B - V$ CMD and a differential reddening map. We obtain an estimate of $E(B - V) = 0.41$ for the foreground reddening towards M4 based on a comparison with M5, a value consistent with previous determinations.

We also studied the variable star V46, discovered by Kaluzny et al. (1997) in the same data set. We present and discuss its spectrum, which indicates that it is a hot subdwarf and present a new light curve, derived with the ISIS image subtraction package (Alard 2000). We also identify two new variables, both lying on the cluster RGB.

W. Landsman, G. Preston, and K.Z. Stanek provided us with helpful comments on the manu-

script. We would like to thank H. Duerbeck for help with the spectroscopic observations, G. Pójmański for *lc* - the light curve analysis utility and N. Samus for the comparison *BV* photometry. We also thank the referee for a very useful report, which significantly improved this paper. BJM, JK and WP were supported by the Polish KBN grant 5P03D004.21. BJM was also supported by the Foundation for Polish Science stipend for young scientists. JK was also supported by the NSF grant AST-9819787. IT was supported by the NSF grant AST-9819786.

REFERENCES

- Alard, C., Lupton, R. 1998 ApJ, 503, 325
- Alard, C. 2000 A&AS, 144, 363
- Alcaino, G., Liller, W., Alvarado, F., Kravtsov, V., Ipatov, A., Samus, N., Smirnov, O. 1997, AJ, 114, 189
- Bellazzini, M., Pecci, F. F., Ferraro, F. R., Galleti, S., Catelan, M. ;., & Landsman, W. B. 2001, AJ, 122, 2569
- Boyle, B. J., Shanks, T., Croom, S. M., Smith, R. J., Miller, L., Loaring, N. & Heymans, C. 2000, MNRAS, 317, 1014
- Breger at al. 1995, A&A, 297, 473
- Carretta, E. & Gratton, R. G. 1997, 121, 95
- Catelan, M. 2000, ApJ, 531, 826
- Chan, E., Richer, H. B. 1986, ApJ, 302, 257
- Cool, A. M. et al. 1998, ApJ, 508, L75
- Cudworth, K. M., Rees, R. 1990, AJ, 99, 1491
- D'Cruz, N. L. 1998, PASP, 110, 1370
- D'Cruz, N. L., et al. 1996, ApJ, 446, 359
- Edmonds, P. D. et al. 1999, ApJ, 516, 250
- Fahlman, G. G.. et al. 1996, ApJ, 459, L65
- Ferraro, F. R., D'Amico, N., Possenti, A., Mignani, R. P., & Paltrinieri, B. 2001, ApJ, 561, 337
- Girardi, L., Bressan, A., Bertelli, G., Chiosi, C. 2000 A&AS, 141, 371
- Harris, W. E. 1996, AJ, 112, 1487
- Hewett, P. C., Foltz, C. B. and Chaffee, F. H. 1995, AJ, 109, 1498

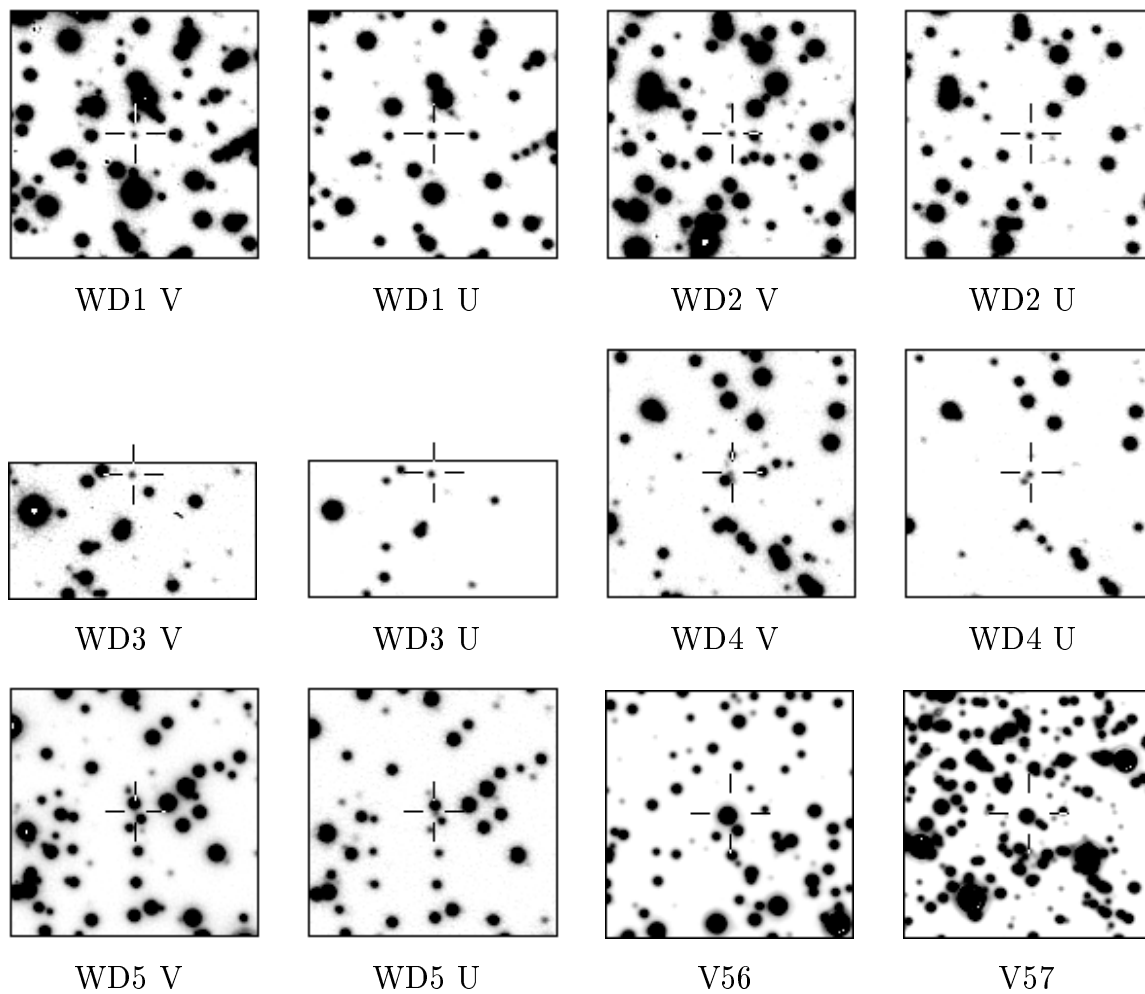


Fig. 13.— Finding charts for the white dwarfs and two new variables, V56 and V57. North is up and east is to the right.

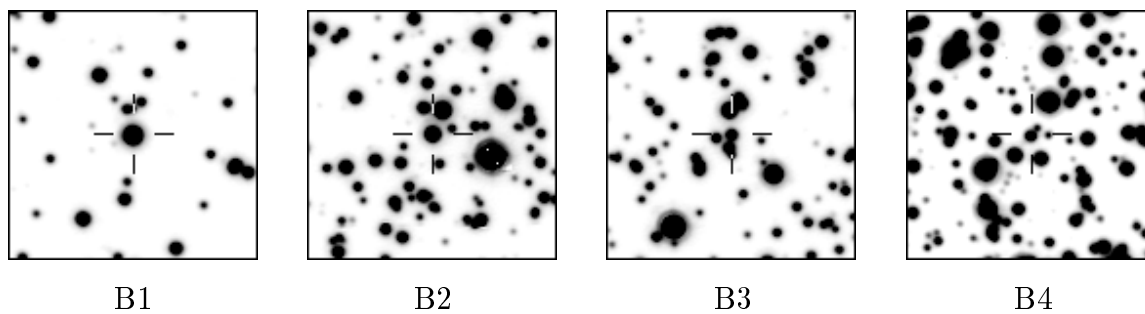


Fig. 14.— Finding charts for the blue subdwarfs. North is up and east is to the right.

- Ibata, R. A., Richer, H. B., Fahlman, G. G., Bolte, M., Bond, H. E., Hesser, J. E., Pryor, C., Stetson, P. B. 1999, *ApJS*, 120, 265
- Ivans, I. I. et al. 1999 *AJ*, 118, 1273
- Ivans, I. I. et al. 2000, preprint (astro-ph/0005595)
- Jeffery, C. S., Drilling, J. S., Harrison, P. M., Heber, U., Moehler, S. 1997, *A&AS*, 125, 501
- Kaluzny, J., Krzeminski, W. 1993, *MNRAS*, 264, 785
- Kaluzny, J., Thompson, I. B., Krzeminski, W. 1997, *AJ*, 113, 2219
- Kaluzny, J. & Thompson, I. B. 2001, *A&A*, 373, 899
- Kaluzny, J., Udalski, A. 1992, *Acta Astron.*, 42, 29
- Koen, C., Kilkenney, D., O'Donoghue, D. and Stobie, R. S. 1998, *IAU Symp.* 185: New Eyes to See Inside the Sun and Stars, 185, 361
- Köhler, T., Groote, D., Reimers, D. and Wisotzki, L. 1997, *A&A*, 325, 502
- Krzeminski, W. 1972, *Acta Astron.*, 22, 387
- Landolt, A. 1992, *AJ*, 104, 340
- Lyons, M. A., Bates, B., Kemp, S. N., Davies, R. D. 1995, *MNRAS*, 277, 113
- Marsh, T. R. 1999, *MNRAS*, 304, 443
- Mochejska, B. J., Kaluzny, J. 1999, *Acta Astron.*, 49, 351
- Moehler, S., Landsman, W., Napiwotzki, R. 1998, *A&A*, 335, 510
- Paczynski, B. 1997, in *The Extragalactic Distance Scale*, ed. M. Livio, M. Donahue & N. Panagia (Cambridge: Cambridge Univ. Press), 273
- Peterson, R. C., Rees, R. F., Cudworth, K. M. 1995, *ApJ*, 443, 124
- Peterson, R. C., Terndrup, D. M., Sadler, E. M., Walker, A. R. 2001, *ApJ*, 547, 240
- Pickles, A. J. 1998, *PASP*, 110, 863
- Provencal et al. 1995, *ApJ*, 445, 927
- Pych, W., Kaluzny, J., Krzeminski, W., Schwarzenberg-Czerny, A., & Thompson, I. B. 2001, *A&A*, 367, 148
- Rich, R. M. et al. 1997 *ApJ*, 484, L25
- Richer, H. B. et al. 1997, *ApJ*, 484, 741
- Richer, H. B. et al. 1995 *ApJ*, 451, L17
- Rosenberg, A., Saviane, I., Piotto, G. & Aparicio, A. 1999, *AJ*, 118, 2306
- Saffer, R. A., Green, E. M., Bowers, T. P. 2000, preprint (astro-ph/0012244)
- Sandquist, E. L., Bolte, M., Stetson, P. B., Hesser, J. E. 1996, *ApJ*, 470, 910
- Schlegel, D. J., Finkbeiner, D. P. & Davis, M. 1998, *ApJ*, 500, 525
- Stetson, P. B. 1994, *PASP*, 106, 250
- von Braun, K. & Mateo, M. 2001, *AJ*, 121, 1522

TABLE 1
LIST OF EXPOSURES

Filter	Exposure Time [s]	FWHM ["]
U	4×900	0.91
	480	1.17
B	2×800	1.01
	3×120	0.91
	30	0.99
V	3×300	0.86
	3×60	1.04
	20	1.09
	6	0.99

TABLE 2
HOT SUBDWARF CANDIDATES IN M4

ID	α_{2000}	δ_{2000}	V	$B - V$	$U - V$
B1	245.84248	-26.46734	15.86	0.06	-0.83
B2	245.85941	-26.52419	16.39	0.09	-0.81
B3	245.86347	-26.54041	17.72	0.13	-0.63
B4	245.89129	-26.50645	19.81	0.01	-0.94

NOTE.—B1=Y435

TABLE 3
LUMINOUS WHITE DWARF CANDIDATES IN M4

ID	α_{2000}	δ_{2000}	V	$B - V$	$U - V$
WD1	245.89291	-26.57736	21.38	0.12	-0.74
WD2	245.94001	-26.55283	21.38	0.23	-0.29
WD3	245.86420	-26.45166	21.76	0.17	-0.69
WD4	245.86497	-26.47151	22.02	0.12	-0.65
WD5	245.84395	-26.55067	22.02	0.13	-0.70

TABLE 4
THE M4 $V/B - V$ FIDUCIAL SEQUENCE

V	$B - V$
13.250	1.285
13.861	1.214
14.430	1.161
15.034	1.118
15.542	1.089
16.029	1.054
16.270	1.010
16.435	0.900
16.550	0.870
16.695	0.860
16.826	0.856
17.056	0.856
17.266	0.866
17.466	0.876
17.706	0.906
17.906	0.926
18.106	0.946
18.316	0.986
18.526	1.016
18.736	1.056
18.976	1.086
19.176	1.126
19.356	1.176
19.606	1.216
19.766	1.266
19.966	1.316
20.116	1.366
20.376	1.416
20.586	1.506
20.796	1.536
20.996	1.616

TABLE 5
OTHER VARIABLES IN M4

ID	α_{2000}	δ_{2000}	P(days)	V_{max}	$B - V$	$U - V$
46	245.94613	-26.53210	0.04358	18.58	0.28	0.28
52	245.88068	-26.51577	0.7765	16.95	0.97	1.27
56	245.89239	-26.49860	...	14.70	1.16	1.68
57	245.90251	-26.53045	...	15.24	1.03	1.48